Original Article

Journal of LOW FREQUENCY NOISE, VIBRATION AND ACTIVE CONTROL

Journal of Low Frequency Noise, Vibration and Active Control
2019, Vol. 38(1) 70–87

DOI: 10.1177/1461348418813255
journals.sagepub.com/home/lfn
SAGE

Torsional vibration of cracked carbon nanotubes with torsional restraints using Eringen's nonlocal differential model

Mustafa Ö Yayli[1], Suheyla Y Kandemir[2] and Ali E Çerçevik[2]

Abstract

Free torsional vibration of cracked carbon nanotubes with elastic torsional boundary conditions is studied. Eringen's nonlocal elasticity theory is used in the analysis. Two similar rotation functions are represented by two Fourier sine series. A coefficient matrix including torsional springs and crack parameter is derived by using Stokes' transformation and nonlocal boundary conditions. This useful coefficient matrix can be used to obtain the torsional vibration frequencies of cracked nanotubes with restrained boundary conditions. Free torsional vibration frequencies are calculated by using Fourier sine series and compared with the finite element method and analytical solutions available in the literature. The effects of various parameters such as crack parameter, geometry of nanotubes, and deformable boundary conditions are discussed in detail.

Keywords

Torsional vibration, cracked carbon nanotubes, Fourier sine series, deformable boundary conditions

Introduction

The simple beam theory extends to the 18th century while the Timoshenko beam theory that allows for the impact of transverse shear deformation was developed in the 20th century. When the classical beam theories are used for the study of micro tubes and nanotubes, they are determined to be insufficient as the theories could not provide the small-scale impact in mechanical properties.[1] Owing to their superior electrical, mechanical, physical, optical, and chemical properties, a great diversity of nanostructures have been formed as a part of nanoelectromechanical and microelectromechanical systems. For such nanoscale structures which cannot be captured by the classical continuum theory. Therefore, a thorough comprehension of the mechanical behavior at nanoscale is very important.[2]

Carbon nanotubes were explored in 1991 by Iijima.[3] Carbon nanotubes are nanomaterials which have tremendous potential in design of new sensors, composite materials, and gas detection. The superior properties of the carbon nanotubes are important instrumental for the improvements in applications.[4–16] Other new fields of application of carbon nanotubes are continuously explored. These nanosized structures[17–21] show that the superior properties such as physical properties, mechanical properties, chemical properties, etc.

Classical continuum theories are frequently used in order to comprehend the mechanical properties of carbon nanotubes.[22–27] The purpose of classical continuum theories may be doubtful in the theoretical analysis of carbon nanotubes, since the theories lack the responsibility of the small-scale effects.[28] Nowadays, many nonclassical continuum theories that integrate material length scales were suggested in the literature to forecast the

[1]Department of Civil Engineering, Faculty of Engineering, Uludag University, Bursa, Turkey
[2]Bilecik SE University, Bilecik, Turkey

Corresponding author:
Mustafa Ö Yayli, Department of Civil Engineering, Faculty of Engineering, Bursa Uludag University, Görükle Campus, Bursa 16059, Turkey.
Email: ozguryayli@uludag.edu.tr

performance of nanostructures. These consist of nonlocal, gradient elasticity, and couple stress theories or composed of the theories.[29–31] Variational formulations and extra boundary conditions within stress gradient elasticity theory with extensions to beam and plate models have been investigated by Polizzotto.[32] Some researchers have investigated the applications of nonlocal elastic models.[33,34]

Nonlocal theories have been used to widely in some papers such as bending, buckling, vibrations, etc. Literature presented that nonlocal elasticity approach[35–43] is a significant technique for modeling mechanical behavior of nanostructures. In the framework of nonlocal elasticity theory, Demir and Civalek[44] have examined the size effects on the torsional vibration of cylindrical tubes,[45] based on the theory of nonlocal continuum mechanics, on the column buckling of multiwalled carbon nanotubes has been investigated. Lu et al.[46] have assessed the multiple shell model and it was improved for the axial buckling of multiwalled carbon nanotubes. Arda and Aydogdu have investigated the statistical torsional deformation and free vibration behaviors of carbon nanotubes. Islam et al.[47] have examined the size effects on the torsional vibration of cylindrical bars. Pradhan and Murmu[48] have reformulated with nonlocal theories the vibration of Euler–Bernoulli beam resting on Winkler elastic foundation. Wang et al.[49] have studied the beam bending solutions based on nonlocal Timoshenko beam theory. A multiple shell model is developed for the axial buckling of multiwalled carbon nanotubes under axial compression by Zhang et al.[50] Free torsional response of cracked nanorods has been explored by several researchers.[51–53] A closed-form model for torsion of nanobeams with an enhanced nonlocal formulation has been proposed by Barretta et al.[54] Different theoretical investigations have been performed for the mechanical behaviors of nanobeams and carbon nanotubes in the literature.[55–58]

In contrast to the rigid supports in which known as free–fixed and fixed–free are not used to describe the exact supporting conditions, the present exact method possesses torsional elastic spring parameters for a better description of real boundary conditions. The classical rigid boundary conditions such as clamped–free, clamped–clamped can be viewed as special cases of the deformable elastic supports.[59] For a clamped support, the dimensionless stiffness value of the torsional spring is infinitely large. For a free edge, the dimensionless stiffness value of the torsional spring is set to be zero. There is strong scientific need to understand the torsional vibration behavior of cracked nanorods in considering the effect of deformable boundary conditions. In this study, free torsional vibration of the cracked nanorods with general elastic spring boundary conditions is investigated on the basis of nonlocal elasticity theory in conjunction with Stokes' transformation.[60,61] The torsional rotation function is represented by a Fourier sine series. A coefficient matrix composed of infinite series is computed by applying a mathematical procedure known as Stokes' transformation to the nonlocal boundary conditions. The determinant of this coefficient matrix gives the torsional vibration frequencies for the cracked nanotubes with torsional restraints.

Background of theory

For homogenous isotropic elastic solids, the Eringen's nonlocal elasticity theory is described by the following theoretical four equations[62]

$$\sigma_{kl,l} + \rho\left(f_l - \frac{\partial^2 u_l}{\partial t^2}\right) = 0 \tag{1}$$

$$\sigma_{kl}(x) = \int_V \alpha\big(|x - x'|, \chi\big)\tau_{kl}(x')\mathrm{d}V(x') \tag{2}$$

$$\tau_{kl}(x') = \lambda\epsilon_{mm}(x')\delta_{kl} + 2\mu\epsilon_{kl}(x') \tag{3}$$

$$\epsilon_{kl}(x') = \frac{1}{2}\left(\frac{\partial u_k(x')}{\partial x'_l} + \frac{\partial u_l(x')}{\partial x'_k}\right) \tag{4}$$

where σ_{kl} denotes the nonlocal stress matrix, ρ represents the mass density of the body, f_l denotes the applied force density to the elastic media, u_l expresses the displacement vector, $\epsilon_{kl}(x')$ represents the strain tensor, V represents the volume occupied by the body, $\tau_{kl}(x')$ expresses the Cauchy stress tensor at any point x', t is the time, μ and λ

denote Lame constants, and $\alpha|x - x'|$ expresses the distance form of Euclidean. $\alpha|x|$ can be expressed by a linear differential operator (ϑ)

$$\vartheta\alpha\big(|x - x'|\big) = \delta\big(|x - x'|\big) \tag{5}$$

the following equation may be derived from equation (2)

$$\vartheta\sigma_{kl} = \tau_{kl} \tag{6}$$

Finally, the following equation can be obtained from equation (1)

$$\tau_{kl,l} + \vartheta(f_l - \rho\ddot{u}_k) = 0 \tag{7}$$

In equation (7), the differential operator proposed by Eringen and Edelen[62] can be written as follows

$$\vartheta = \left[1 - (e_0 a)^2 \nabla^2\right] \tag{8}$$

where a expresses internal length, e_0 denotes the material constant, and ∇^2 represents the Laplacian. The following constitutive equation can be obtained in terms of nonlocal parameter

$$\left[1 - (e_0 a)^2 \nabla^2\right]\sigma_{kl} = \tau_{kl} \tag{9}$$

For nonlocal elasticity problems formulated in unbounded domains (free–free boundary conditions or elastic boundaries), differential law model by Eringen and Edelen[62] may be considered equivalent to a stress and strain-driven model, due to the tacit fulfillment of nonlocal boundary conditions of vanishing at infinity. So, differential equation model by Eringen and Edelen[62] is effectively exploited to explore Rayleigh surface waves and screw dislocations. Using Eringen's nonlocal elasticity theory with exponential kernel, there are constitutive boundary conditions and paradoxes in nonlocal elastic nanobeams.[63] They have recently showed the ill-posedness of the Eringen integral model and exact solutions of inflected functionally graded nanobeams in integral elasticity. Barretta et al.[64] have examined the exact solutions of inflected functionally graded nanobeams in integral elasticity.

Formulation of the problem

The equation of motion of torsional vibration problem in nonlocal elasticity is given as follows[44]

$$GJ\frac{\partial^2\theta(x,t)}{\partial x^2} - \left\{1 - (e_0 a)^2 \frac{\partial^2}{\partial x^2}\right\}\rho J\frac{\partial^2\theta(x,t)}{\partial t^2} = 0 \tag{10}$$

Due to the fact that the crack separates the carbon nanotube into two parts, rotation function may not be shown by a single torsional function, so that two rotation functions are used in this section. It can be seen in Figure 1 that nanotube is assumed to be divided into two parts by the crack. Therefore, equation (10) can be rewritten as

$$0 < x < l_1 \quad GJ\frac{\partial^2\theta_1(x,t)}{\partial x^2} - \left\{1 - (e_0 a)^2 \frac{\partial^2}{\partial x^2}\right\}\rho J\frac{\partial^2\theta_1(x,t)}{\partial t^2} = 0 \tag{11}$$

$$l_1 < x < L \quad GJ\frac{\partial^2\theta_2(x,t)}{\partial x^2} - \left\{1 - (e_0 a)^2 \frac{\partial^2}{\partial x^2}\right\}\rho J\frac{\partial^2\theta_2(x,t)}{\partial t^2} = 0 \tag{12}$$

Modal displacement function

It has been widely accepted that it is very difficult to calculate an exact analytical solution for the cracked nanorods, except for rigid boundary conditions (clamped–free and clamped–clamped). In this paper, a torsional spring is utilized to substitute the effect of crack on the free vibration. The rotations are denoted by $\theta_1(x,t)$ and $\theta_2(x,t)$. Assuming harmonic vibrations, $\theta_1(x,t)$ and $\theta_2(x,t)$ can be expressed in the following form

$$\theta_1(x,t) = \xi(x)\cos(\Omega t) \tag{13}$$

$$\theta_2(x,t) = \zeta(x)\cos(\Omega t) \tag{14}$$

where $\xi(x)$ and $\zeta(x)$ are the rotation functions about the center of twist and Ω is the natural frequency of the problem. The modal rotation functions both $\xi(x)$ and $\zeta(x)$ can be described in three regions as follows

$$\xi(x) = \begin{bmatrix} \xi_0 & x = 0 \\ \xi_{l_1} & x = l_1 \\ \sum_{n=1}^{\infty} A_n \sin(\alpha_n x) & 0 < x < l_1 \end{bmatrix} \tag{15}$$

$$\zeta(x) = \begin{bmatrix} \zeta_0 & x = l_1 \\ \zeta_{l_2} & x = L \\ \sum_{n=1}^{\infty} B_n \sin(\beta_n x) & l_1 < x < L \end{bmatrix} \tag{16}$$

where

$$\alpha_n = \frac{n\pi x}{l_1} \tag{17}$$

$$\beta_n = \frac{n\pi x}{l_2} \tag{18}$$

The coefficients (A_n) in equation (15) can be written as

$$A_n = \frac{2}{l_1}\int_0^{l_1} \xi(x)\sin(\alpha_n x)\mathrm{d}x \tag{19}$$

Taking the first derivative of equation (15) yields[65]

$$\xi'(x) = \sum_{n=1}^{\infty} \alpha_n A_n \cos(\alpha_n x) \tag{20}$$

Fourier cosine series can be used for equation (20) as follows

$$\xi'(x) = \frac{f_0}{l_1} + \sum_{n=1}^{\infty} f_n \cos(\alpha_n x) \tag{21}$$

The following coefficients can be found

$$f_0 = \frac{2}{l_1}\int_0^{l_1} \xi'(x)\mathrm{d}x = \frac{2}{l_1}[\xi(l_1) - \xi(0)] \tag{22}$$

$$f_n = \frac{2}{l_1}\int_0^{l_1} \xi'(x)\cos(\alpha_n x)\mathrm{d}x \quad n = 1, 2\ldots \tag{23}$$

By using the integration by parts rule

$$f_n = \frac{2}{l_1}[\xi(x)\cos(\alpha_n x)]_0^{l_1} + \frac{2}{l_1}\left[\alpha_n\int_0^{l_1} \xi(x)\sin(\alpha_n x)\mathrm{d}x\right] \tag{24}$$

$$f_n = \frac{2}{l_1}\left[(-1)^n\xi(l_1) - \xi(0)\right] + \alpha_n A_n \tag{25}$$

The first two derivatives of the selected function can be obtained by employing Stokes' transformation as follows

$$\frac{d\xi(x)}{dx} = \frac{\xi_{l_1} - \xi_0}{l_1} + \sum_{n=1}^{\infty}\cos(\alpha_n x)\left(\frac{2\left((-1)^n\xi_{l_1} - \xi_0\right)}{l_1} + \alpha_n A_n\right) \tag{26}$$

$$\frac{d^2\xi(x)}{dx^2} = -\sum_{n=1}^{\infty}\alpha_n\sin(\alpha_n x)\left(\frac{2\left((-1)^n\xi_{l_1} - \xi_0\right)}{l_1} + \alpha_n A_n\right) \tag{27}$$

Similarly, the first and second derivatives of equation (16) can be calculated with the use of the above algorithm[66]

$$\frac{d\zeta(x)}{dx} = \frac{\zeta_{l_2} - \zeta_0}{l_2} + \sum_{n=1}^{\infty}\cos(\beta_n x)\left(\frac{2\left((-1)^n\zeta_{l_2} - \zeta_0\right)}{l_2} + \beta_n B_n\right) \tag{28}$$

$$\frac{d^2\zeta(x)}{dx^2} = -\sum_{n=1}^{\infty}\beta_n\sin(\beta_n x)\left(\frac{2\left((-1)^n\zeta_{l_2} - \zeta_0\right)}{l_2} + \beta_n B_n\right) \tag{29}$$

Substituting equations (13), (14), (27), and (29) into equations (11) and (12), the coefficients A_n and B_n can be obtained in terms of ξ_0, ξ_{l_1}, ζ_0, and ζ_{l_2} as follows

$$A_n = \frac{2}{l_1}\frac{(l_1^2 - \varpi_1^2(e_0a)^2)\alpha_n\left(\xi_0 - (-1)^n\xi_{l_1}\right)}{-\varpi_1^2 + (l_1^2 - \varpi_1^2(e_0a)^2)\alpha_n^2} \tag{30}$$

$$B_n = \frac{2}{l_2}\frac{(l_2^2 - \varpi_2^2(e_0a)^2)\beta_n\left(\zeta_0 - (-1)^n\zeta_{l_2}\right)}{-\varpi_2^2 + (l_2^2 - \varpi_2^2(e_0a)^2)\beta_n^2} \tag{31}$$

where

$$\varpi_1^2 = \frac{\rho\Omega^2 l_1^2}{G} \tag{32}$$

$$\varpi_2^2 = \frac{\rho\Omega^2 l_2^2}{G} \tag{33}$$

The formulations of the rotations for two parts become

$$\theta_1(x,t)=\sum_{n=1}^{\infty}\frac{2}{l_1}\frac{\Delta_1\alpha_n\left(\xi_0-(-1)^n\xi_{l_1}\right)}{-\varpi_1^2+\Delta_1\alpha_n^2}\cos(\Omega t)\sin(\alpha_n x) \tag{34}$$

$$\theta_2(x,t)=\sum_{n=1}^{\infty}\frac{2}{l_2}\frac{\Delta_2\beta_n\left(\zeta_0-(-1)^n\zeta_{l_2}\right)}{-\varpi_2^2+\Delta_2\beta_n^2}\cos(\Omega t)\sin(\beta_n x) \tag{35}$$

where

$$\Delta_1=l_1^2-\varpi_1^2(e_0a)^2 \tag{36}$$

$$\Delta_2=l_2^2-\varpi_2^2(e_0a)^2 \tag{37}$$

Nonlocal boundary conditions

A carbon nanotube with length L and one crack is located as in Figure 1. Then the following relation can be written

$$L=l_1+l_2 \tag{38}$$

It is assumed that the crack is located at point l_1 from the origin of axes. The carbon nanotube is divided into two segments with lengths l_1, l_2. Using equations (9) and (10), the nonlocal torque T can be written as

$$T=\left[GJ+(e_0a)^2m\frac{\partial}{\partial t^2}\right]\frac{\partial\theta(x,t)}{\partial x} \tag{39}$$

It may be derived from equation (39) that the nonlocal boundary conditions at the torsional spring points can be expressed as

$$\phi_0\xi_0=\left[GJ+(e_0a)^2m\frac{\partial}{\partial t^2}\right]\frac{\partial\theta_1(x,t)}{\partial x},\quad x=0 \tag{40}$$

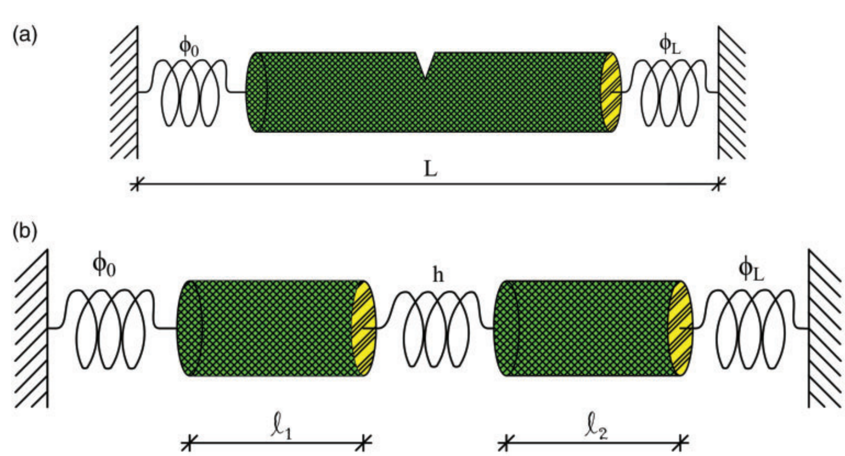

Figure 1. Modeling of a cracked nanotube with torsional restraints.

$$\phi_L \zeta_{l_2} = -\left[GJ + (e_0 a)^2 m \frac{\partial}{\partial t^2}\right] \frac{\partial \theta_2(x,t)}{\partial x}, \quad x = L \tag{41}$$

where ϕ_0, ϕ_L are the stiffnesses of the torsional springs at the ends of the carbon nanotube. The jump conditions can be conveniently written as

$$h(\xi_{l_1} - \zeta_0) = -\left[GJ + (e_0 a)^2 m \frac{\partial}{\partial t^2}\right] \frac{\partial \theta_1(l_1,t)}{\partial x}, \quad x = l_1 \tag{42}$$

$$\frac{\partial \theta_1(l_1,t)}{\partial x} = \frac{\partial \theta_2(0,t)}{\partial x}, \quad x = l_1 \tag{43}$$

where h is the crack flexibility parameter. After some mathematical operations, the substitution of equations (13), (14), (26), and (28) into equations (40) to (43) leads to the four equations as follows

$$\left(-\Delta_1\Phi_0 + \gamma^2\lambda^2 - 1 + \sum_{n=1}^{\infty} \frac{2\Delta_1^2\lambda^2 - 2\gamma^2\Delta_1^2\lambda^4}{-\Delta_1^2\lambda^2 - \pi^2\gamma^2\lambda^2 n^2 + \pi^2 n^2}\right)\xi_0 + \left(1 - \gamma^2\lambda^2 + \sum_{n=1}^{\infty} \frac{2\gamma^2\Delta_1^2\lambda^4(-1)^n - 2\Delta_1^2\lambda^2(-1)^n}{-\Delta_1^2\lambda^2 - \pi^2\gamma^2\lambda^2 n^2 + \pi^2 n^2}\right)\xi_{l_1} = 0 \tag{44}$$

$$\left(1 - \gamma^2\lambda^2 + \sum_{n=1}^{\infty} \frac{2\gamma^2\Delta_2^2\lambda^4(-1)^n - 2\Delta_2^2\lambda^2(-1)^n}{-\Delta_2^2\lambda^2 - \pi^2\gamma^2\lambda^2 n^2 + \pi^2 n^2}\right)\zeta_0 + \left(\gamma^2\lambda^2 - \Delta_2\Phi_L - 1 \quad + \sum_{n=1}^{\infty} \frac{2\Delta_2^2\lambda^2 - 2\gamma^2\Delta_2^2\lambda^4}{-\Delta_2^2\lambda^2 - \pi^2\gamma^2\lambda^2 n^2 + \pi^2 n^2}\right)\zeta_{l_2} = 0 \tag{45}$$

$$\begin{gathered}\left(\gamma^2\lambda^2 - 1 + \sum_{n=1}^{\infty} \frac{2\Delta_1^2\lambda^2 - 2\gamma^2\Delta_1^2\lambda^4}{-\Delta_1^2\lambda^2 - \pi^2\gamma^2\lambda^2 n^2 + \pi^2 n^2}\right)\xi_0 \\ + (-\gamma^2\lambda^2 + \frac{\delta_1}{K} + 1 + \sum_{n=1}^{\infty} \frac{2\gamma^2\Delta_1^2\lambda^4(-1)^n - 2\Delta_1^2\lambda^2(-1)^n}{-\Delta_1^2\lambda^2 - \pi^2\gamma^2\lambda^2 n^2 + \pi^2 n^2})\xi_{l_1} - \frac{\Delta_1}{K}\zeta_0 = 0\end{gathered} \tag{46}$$

$$\begin{gathered}\left(-\frac{1}{\Delta_1} + \sum_{n=1}^{\infty} \frac{2\Delta_1\lambda^2(-1)^n}{-\Delta_1^2\lambda^2 - \pi^2\gamma^2\lambda^2 n^2 + \pi^2 n^2}\right)\xi_0 + \left(\frac{1}{\Delta_1} - \sum_{n=1}^{\infty} \frac{2\Delta_1\lambda^2}{-\Delta_1^2\lambda^2 - \pi^2\gamma^2\lambda^2 n^2 + \pi^2 n^2}\right)\xi_{l_1} \\ + \left(\frac{1}{\Delta_2} - \sum_{n=1}^{\infty} \frac{2\Delta_2\lambda^2}{-\Delta_2^2\lambda^2 - \pi^2\gamma^2\lambda^2 n^2 + \pi^2 n^2}\right)\zeta_0 + \left(-\frac{1}{\Delta_2} - \sum_{n=1}^{\infty} \frac{2\Delta_2\lambda^2(-1)^n}{-\Delta_2^2\lambda^2 - \pi^2\gamma^2\lambda^2 n^2 + \pi^2 n^2}\right)\zeta_{l_2} = 0\end{gathered} \tag{47}$$

where

$$\gamma = \frac{e_0 a}{L} \tag{48}$$

$$K = \frac{GJ}{hL} \tag{49}$$

$$\Delta_1 = \frac{l_1}{L} \tag{50}$$

$$\Delta_2 = \frac{l_2}{L} \tag{51}$$

$$\Phi_0 = \frac{\phi_0 L}{GJ} \tag{52}$$

$$\Phi_L = \frac{\phi_L L}{GJ} \tag{53}$$

$$\lambda = \sqrt{\frac{\rho\omega^2 L^2}{G}} \tag{54}$$

and the following system of equations is obtained in a matrix form

$$\begin{bmatrix} \psi_{11} & \psi_{12} & \psi_{13} & \psi_{14} \\ \psi_{21} & \psi_{22} & \psi_{23} & \psi_{24} \\ \psi_{31} & \psi_{32} & \psi_{33} & \psi_{34} \\ \psi_{41} & \psi_{42} & \psi_{43} & \psi_{44} \end{bmatrix} \begin{bmatrix} \xi_0 \\ \xi_{l_1} \\ \zeta_0 \\ \zeta_{l_2} \end{bmatrix} = 0 \tag{55}$$

where

$$\psi_{11} = -\Delta_1\Phi_0 + \gamma^2\lambda^2 - 1 + \sum_{n=1}^{\infty} \frac{2\Delta_1^2\lambda^2 - 2\gamma^2\Delta_1^2\lambda^4}{-\Delta_1^2\lambda^2 - \pi^2\gamma^2\lambda^2 n^2 + \pi^2 n^2} \tag{56}$$

$$\psi_{12} = 1 - \gamma^2\lambda^2 + \sum_{n=1}^{\infty} \frac{2\gamma^2\Delta_1^2\lambda^4(-1)^n - 2\Delta_1^2\lambda^2(-1)^n}{-\Delta_1^2\lambda^2 - \pi^2\gamma^2\lambda^2 n^2 + \pi^2 n^2} \tag{57}$$

$$\psi_{13} = 0 \quad \psi_{14} = 0 \quad \psi_{21} = 0 \quad \psi_{22} = 0 \tag{58}$$

$$\psi_{23} = 1 - \gamma^2\lambda^2 + \sum_{n=1}^{\infty} \frac{2\gamma^2\Delta_2^2\lambda^4(-1)^n - 2\Delta_2^2\lambda^2(-1)^n}{-\Delta_2^2\lambda^2 - \pi^2\gamma^2\lambda^2 n^2 + \pi^2 n^2} \tag{59}$$

$$\psi_{24} = \gamma^2\lambda^2 - \Delta_2\Phi_L - 1 + \sum_{n=1}^{\infty} \frac{2\delta_2^2\lambda^2 - 2\gamma^2\Delta_2^2\lambda^4}{-\Delta_2^2\lambda^2 - \pi^2\gamma^2\lambda^2 n^2 + \pi^2 n^2} \tag{60}$$

$$\psi_{31} = \gamma^2\lambda^2 - 1 + \sum_{n=1}^{\infty} \frac{2\Delta_1^2\lambda^2 - 2\gamma^2\Delta_1^2\lambda^4}{-\Delta_1^2\lambda^2 - \pi^2\gamma^2\lambda^2 n^2 + \pi^2 n^2} \tag{61}$$

$$\psi_{32} = -\gamma^2\lambda^2 + \frac{\Delta_1}{K} + 1 + \sum_{n=1}^{\infty} \frac{2\gamma^2\delta_1^2\lambda^4(-1)^n - 2\Delta_1^2\lambda^2(-1)^n}{-\Delta_1^2\lambda^2 - \pi^2\gamma^2\lambda^2 n^2 + \pi^2 n^2} \tag{62}$$

$$\psi_{33} = -\frac{\Delta_1}{K} \quad \psi_{34} = 0 \tag{63}$$

$$\psi_{41} = -\frac{1}{\Delta_1} + \sum_{n=1}^{\infty} \frac{2\Delta_1\lambda^2(-1)^n}{-\Delta_1^2\lambda^2 - \pi^2\gamma^2\lambda^2 n^2 + \pi^2 n^2} \tag{64}$$

$$\psi_{42} = \frac{1}{\Delta_1} - \sum_{n=1}^{\infty} \frac{2\Delta_1\lambda^2}{-\Delta_1^2\lambda^2 - \pi^2\gamma^2\lambda^2 n^2 + \pi^2 n^2} \tag{65}$$

$$\psi_{43} = \frac{1}{\Delta_2} - \sum_{n=1}^{\infty} \frac{2\Delta_2\lambda^2}{-\Delta_2^2\lambda^2 - \pi^2\gamma^2\lambda^2 n^2 + \pi^2 n^2} \tag{66}$$

$$\psi_{44} = -\frac{1}{\Delta_2} - \sum_{n=1}^{\infty} \frac{2\Delta_2 \lambda^2 (-1)^n}{-\Delta_2^2 \lambda^2 - \pi^2 \gamma^2 \lambda^2 n^2 + \pi^2 n^2} \tag{67}$$

The eigenvalues (λ_n) are obtained by setting the determinant of the matrix in equation (55) to 0

$$|\psi_{ij}| = 0 \quad (i, j = 1, 2, 3, 4) \tag{68}$$

Numerical results and discussion

In this section, some typical examples are solved to demonstrate the validity of the proposed solution, also quantifying the effects of the nonlocal parameter γ with crack parameter K on the vibrational response of nanotubes. The computed results are obtained using 160 terms in series in equation (68).

Verification studies

In order to validate the presented method, as well as to demonstrate their implementation to dynamical analysis, a cracked nanotube with hard torsional springs is considered. The torsional springs are taken as $\Phi_0 = \Phi_L = 10,000$ (for the higher torsional spring coefficients, this problem turns into the clamped–clamped nanotube). The crack parameter K is taken as 0.000001 for noncracked nanotube. The comparison results for the torsional vibration frequencies of the noncracked nanotube for different torsional vibration modes are tabulated in Table 1. It can be seen that the present results are in good agreement with the finite element method and literature.[44] In the second verification study, crack K and one of the torsional spring Φ_0 parameters are similar to the first example and the other torsional spring parameter Φ_L is taken as zero. The comparison studies are tabulated in Table 2. The results are in good agreement with those obtained from previous studies.[44]

Table 1. Comparison of the first three torsional frequency parameters of a nanotube with clamped–clamped.

	Clamped–clamped		$S_0 = S_L = 10^9$
	FEM	Demir and Civalek[44]	Present
Mode	λ_i	λ_i	λ_i
1	3,141	3,141	3.14259
2	6.284	6.283	6.28095
3	9.425	9.424	9.42368

FEM: finite element method.

Table 2. Comparison of the first three frequency parameters of nanorod with clamped–free ends.

	Clamped–free		$S_0 = 10^9$, $S_L = 0$
	FEM	Demir and Civalek[44]	Present
Mode	λ_i	λ_i	λ_i
1	1.571	1.570	1.57539
2	4.712	4.712	4.73481
3	7.854	7.853	7.85398

FEM: finite element method.

Effect of crack location and severity

In a fixed–fixed nanorod with a crack, according to equations (44) to (47), so equation (68) will be simplified to following equation

$$\begin{vmatrix} \psi_{33} & \psi_{34} \\ \psi_{43} & \psi_{44} \end{vmatrix} = 0 \tag{69}$$

In this section the effect of crack location and severity on the first vibration frequency is investigated by using equations (68) and (69). It can be seen from Figures 2 to 5 that by decreasing crack severity K (i.e. the carbon nanotube becomes stiffer), first torsional frequencies decrease for the constant value of nonlocal parameter. It is clearly shown in Figures 2 to 5 that the effect of crack severity is decreased by increasing small-scale parameter. Figures 4 and 5 show the effect of the Δ_1 and Δ_2 parameter on the torsional frequencies highly depends on its location on the carbon nanotube. It can be concluded from these figures that by increasing the values of crack severity K torsional frequencies increase. When the crack location becomes closer to the fixed–fixed end, a larger decrease in the torsional frequencies is observed. The effect of the crack severity parameter on the free torsional

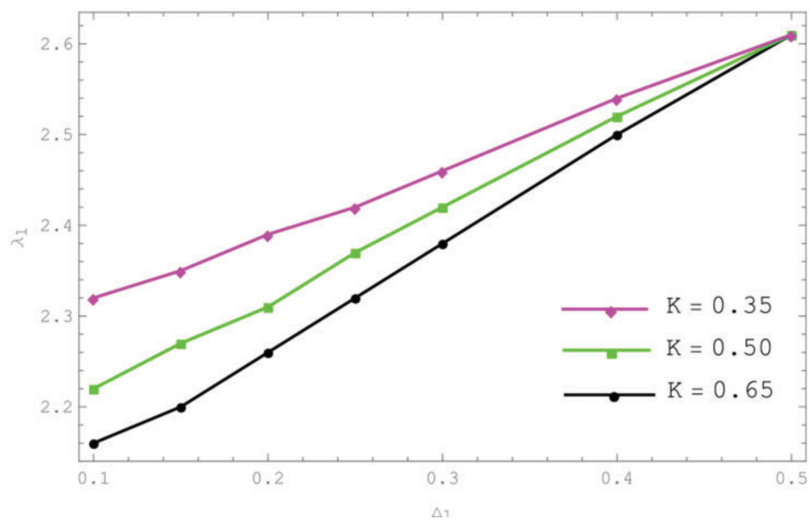

Figure 2. First vibration frequencies as a function of crack location parameter Δ_1 for constant value of nonlocal parameter $\gamma = 0.2$

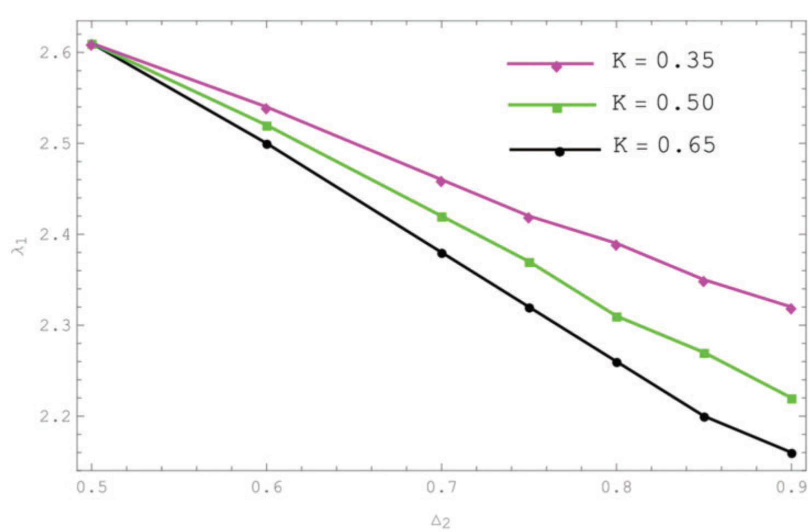

Figure 3. First vibration frequencies as a function of crack location parameter Δ_1 for constant value of nonlocal parameter $\gamma = 0.2$

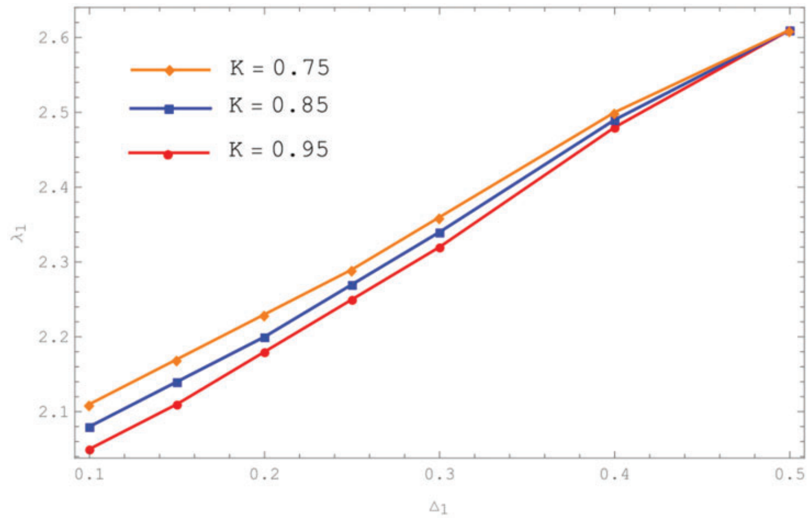

Figure 4. First vibration frequencies as a function of crack location parameter Δ_1 for different crack parameters.

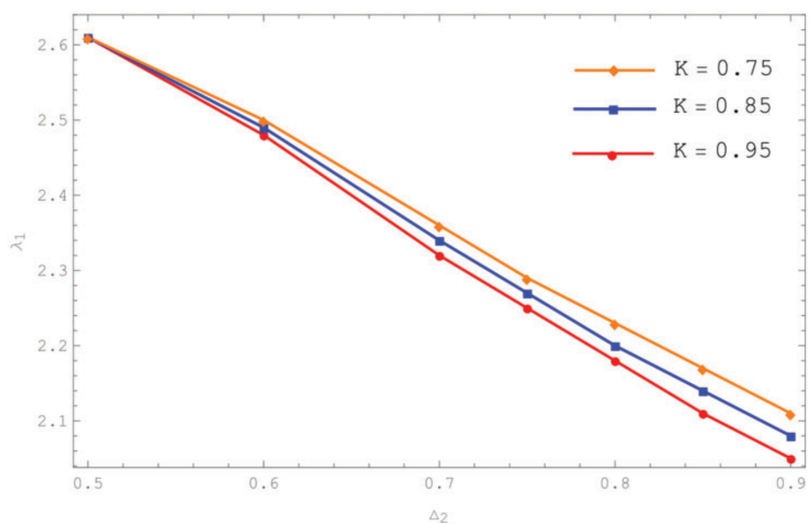

Figure 5. First vibration frequencies as a function of crack location parameter Δ_2 for different crack parameters.

vibration characteristics of the carbon nanotube is also demonstrated in Figures 6 and 7. The increasing value of crack severity coefficient leads to a decrease in the magnitude of the first torsional frequency. It is also noticed from Figures 6 and 7 that the increasing value of the crack location parameter (Δ_1) decreases the stiffness of the carbon nanotube.

Effect of nonlocal parameter

In this subsection, to delineate the effect of small-scale parameter, some numerical case studies are implemented and assessed for the torsional vibration analysis of cracked nanorods, using the derived formulations in the "Formulation of the problem" section. As it is seen from Figures 8 to 14, the first torsional vibration frequency is affected by the nonlocal parameter. This observation is rational, because the torsional rotation is neglected in the clamped–clamped ends and it makes the carbon nanotube behavior invalidly stiffer than the reality. It can be noted that the results predicted by the nonlocal elasticity theory are always greater than those of the classical beam theory. It can be said that the difference among the predicted values is diminishing when the length of the carbon nanotube becomes larger, thereby indicating that the size effect is only significant when the length of the single-walled carbon nanotube is comparable to the nonlocal parameter.

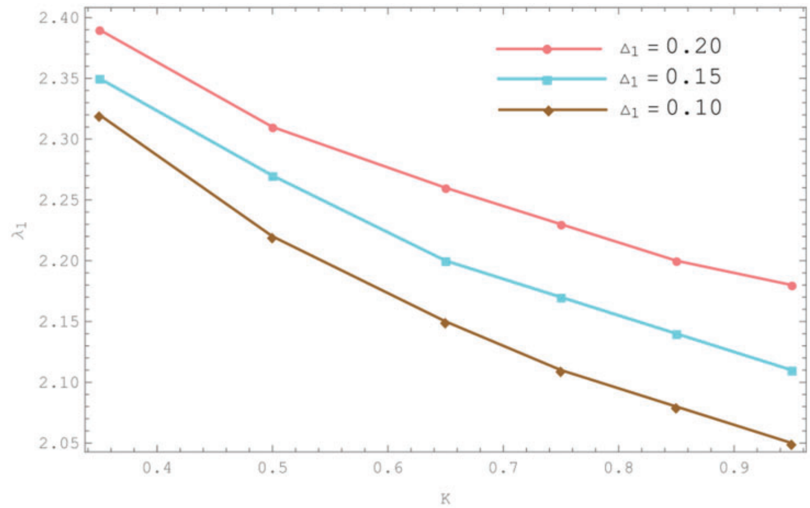

Figure 6. First torsional vibration frequency as a function of crack severity for $\Delta_1 = 0.10, 0.15, 0.20.$

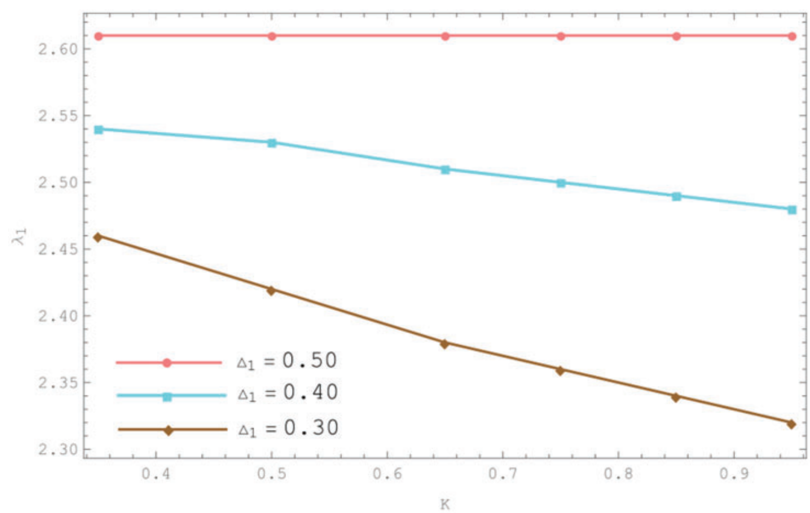

Figure 7. First torsional vibration frequency as a function of crack severity for $\Delta_1 = 0.30, 0.40, 0.50.$

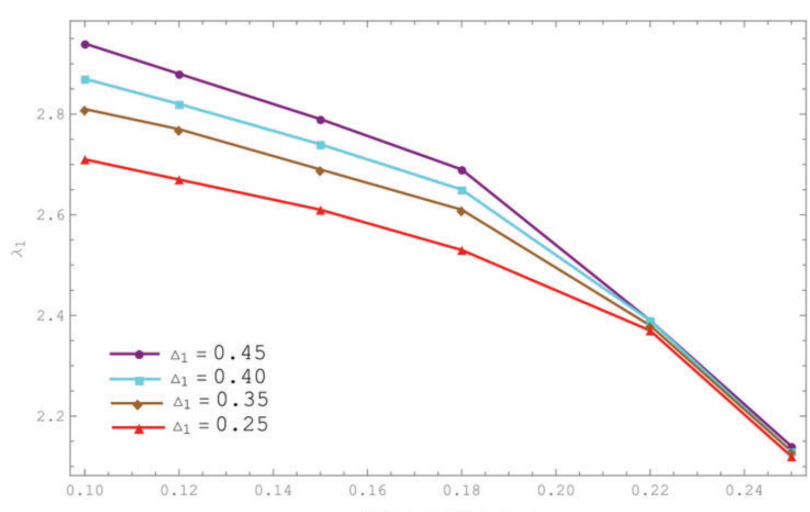

Figure 8. First torsional vibration frequency as a function of nonlocal parameter for $K = 0.25$.

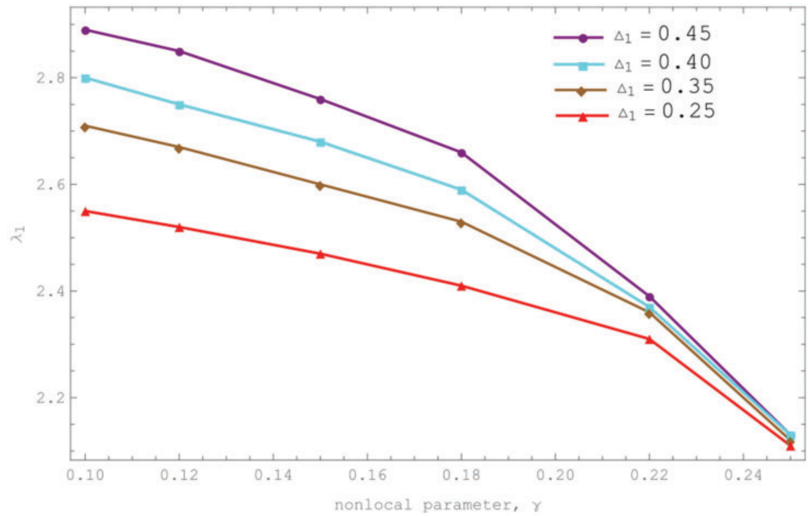

Figure 9. First torsional vibration frequency as a function of nonlocal parameter for $K = 0.50$.

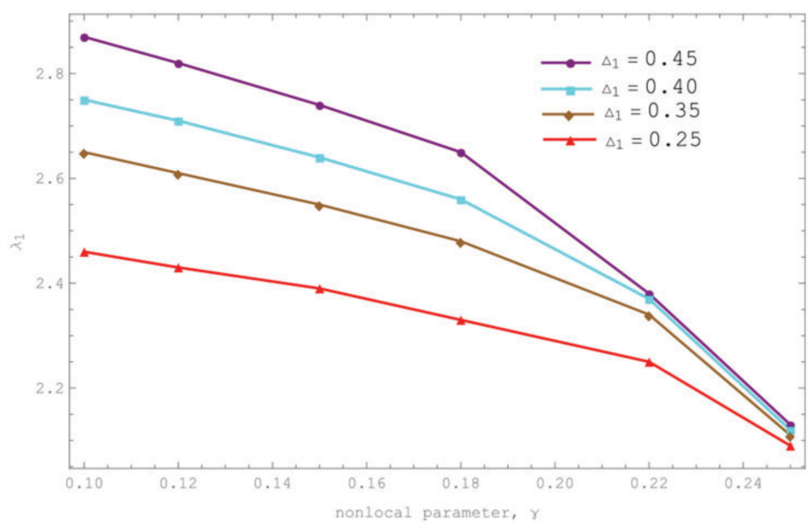

Figure 10. First torsional vibration frequency as a function of nonlocal parameter for $K = 0.75$.

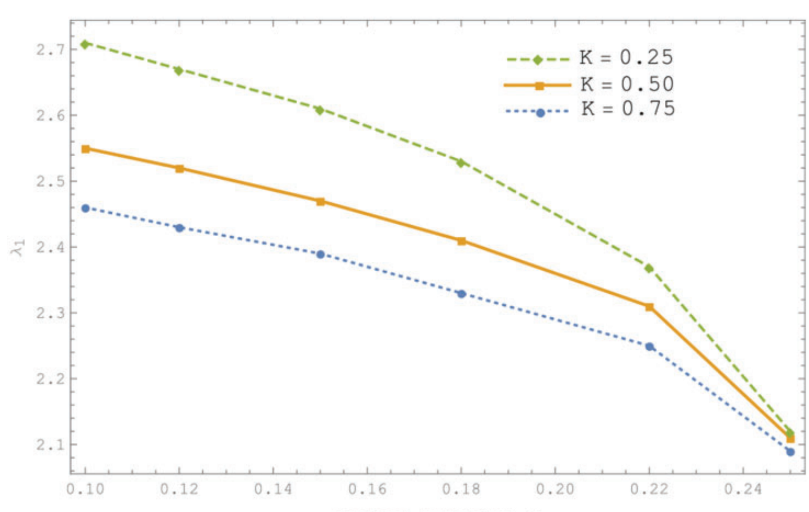

Figure 11. First torsional vibration frequency as a function of nonlocal parameter for $\Delta_1 = 0.25$.

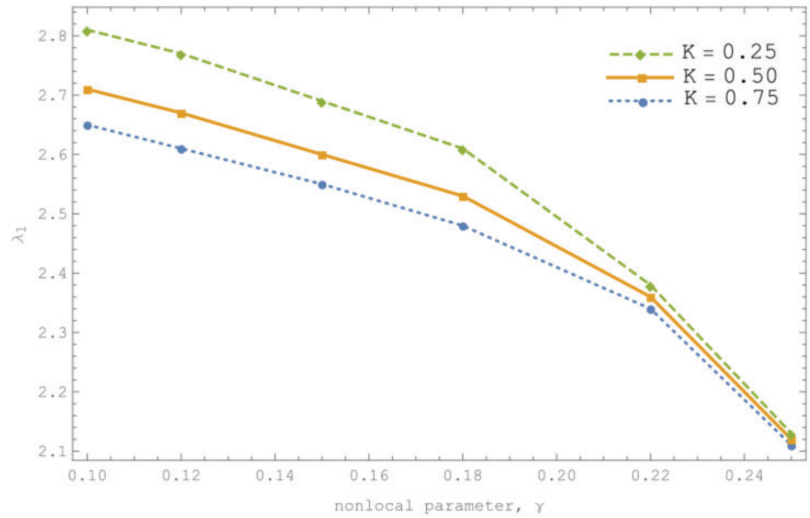

Figure 12. First torsional vibration frequency as a function of nonlocal parameter for $\Delta_1 = 0.35$.

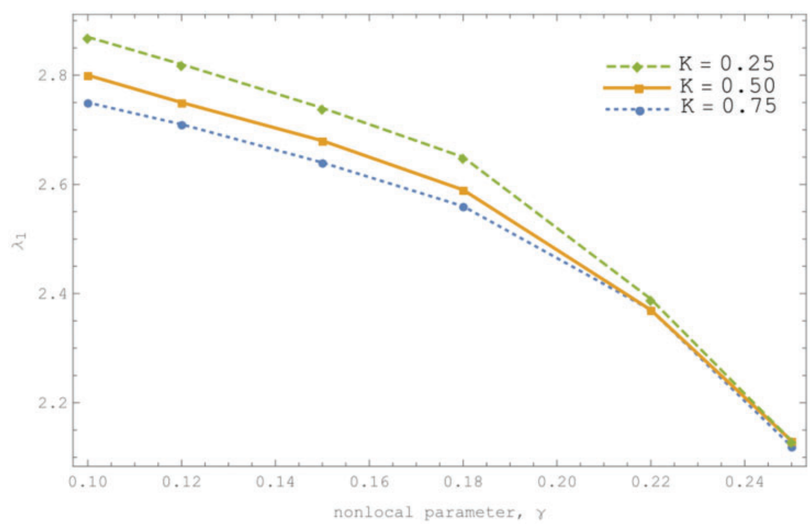

Figure 13. First torsional vibration frequency as a function of nonlocal parameter for $\Delta_1 = 0.40$.

Effect of elastic boundary conditions

In the following example, the effect of elastic medium parameter on the dimensionless vibration frequencies is illustrated in Figure 15(a) to (d). The following mathematical relation is introduced to give a better illustration of the deformable boundary conditions

$$\Gamma_k = \Omega_k^{NL}/\Omega_k^L \tag{70}$$

in which Γ_k is used as the nondimensional frequencies. The index (L) expresses the local elasticity theory ($e_0a = 0$) and (NL) indicates the nonlocal elasticity ($e_0a \neq 0$). In Figure 15, a comparison between nondimensional torsional frequencies of the cracked nanorods with elastic torsional springs at both ends, subjected to different elastic spring parameters $\Phi_0 = \Phi_L = 1, 10, 50, 200$ and constant crack parameter ($K = 0.00001$) is presented for various values of the length and nonlocal parameters based on Fourier series method. It can be observed that the dimensionless first six frequencies decrease by increasing torsional spring parameters and it can be stated that elastic torsional spring parameters have a notable effect on the torsional frequencies of the cracked nanorod.

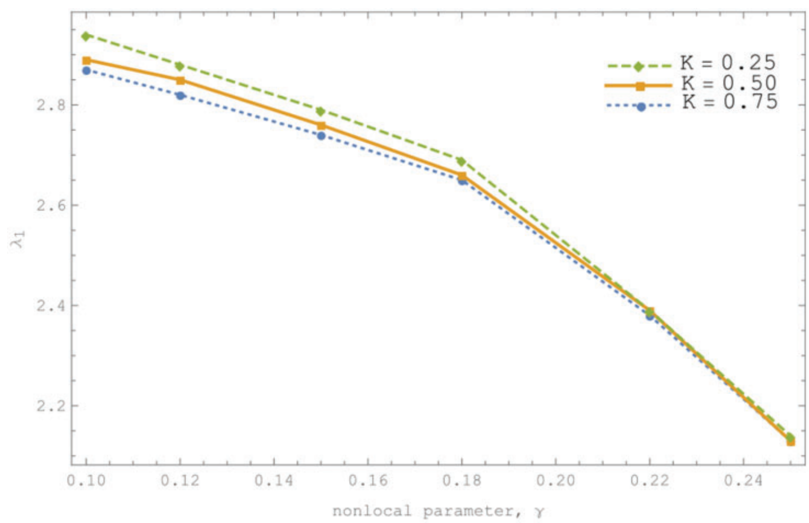

Figure 14. First torsional vibration frequency as a function of nonlocal parameter for $\Delta_1 = 0.45$.

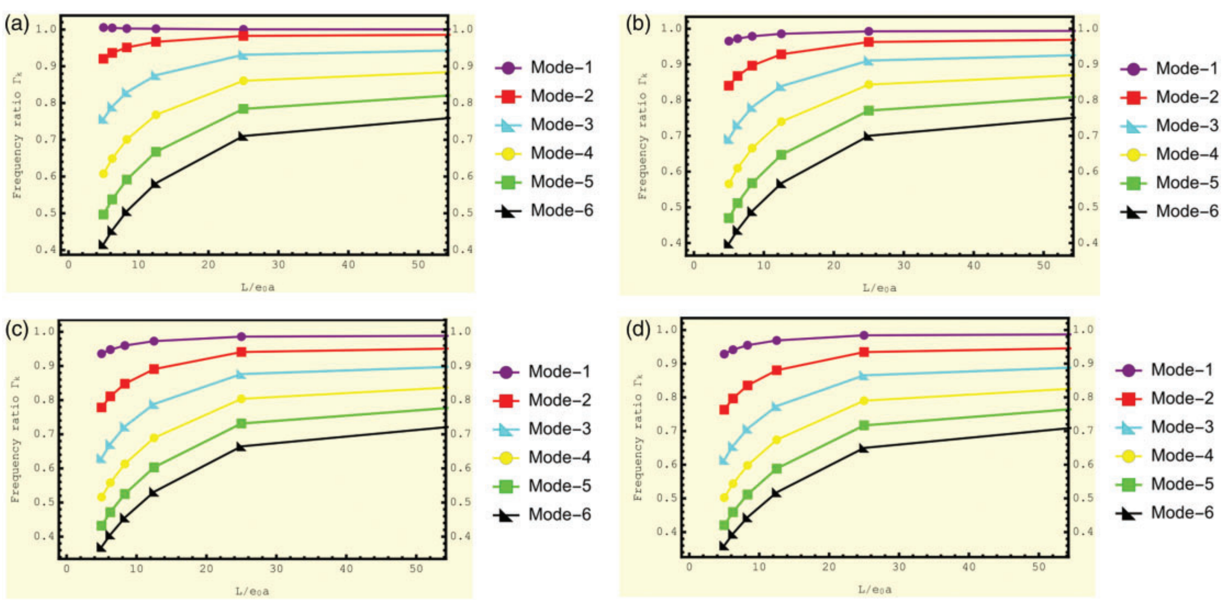

Figure 15. The effect of elastic spring coefficients (Φ_0, Φ_L) on the torsional vibration frequencies.

Conclusion

Due to few detailed studies on the torsional vibration analysis of cracked nanotubes with deformable boundary conditions are available, in the current work, a transformation known as "Stokes' transformation" is applied to the nonlocal elastic boundary conditions. This method gives more flexibility in supporting conditions. It is aimed to construct an exact method for torsional vibration of cracked nanotubes with deformable boundary conditions. A useful coefficient matrix including infinite series is presented for the first time in order to calculate the torsional frequencies. The accuracy of the proposed method, in deriving the torsional vibration frequencies, has been examined by means of numerical example problems. The effects of different parameters are discussed in detail.

It is found that most of the previous studies on the torsional vibration analysis of cracked nanorods have been conducted based on the ignorance of the deformable boundary conditions. As a result, the previous works cannot be utilized in order to thoroughly study the cracked nanorods under investigation. Motivated by this fact, in this work, torsional vibration characteristics of nanorods considering the effects of elastic spring boundary conditions are analyzed. Finally, through some numerical examples, the effect of nonlocal, crack and elastic spring parameters is investigated. It is concluded that various factors such as crack parameter, torsional spring constants, and nonlocal parameter play important roles in free torsional vibration response of nanorod.

Declaration of conflicting interests

The author(s) declared no potential conflicts of interest with respect to the research, authorship, and/or publication of this article.

Funding

The author(s) received no financial support for the research, authorship, and/or publication of this article.

ORCID iD

Mustafa Ö Yayli http://orcid.org/0000-0003-2231-170X

References

1. Wang CM, Zhang YY, Ramesh SS, et al. Buckling analysis of micro- and nano-rods/tubes based on nonlocal Timoshenko beam theory. *J Phys D Appl Phys* 2006; 39: 3904.
2. Zhu X and Li L. Longitudinal and torsional vibrations of size-dependent rods via nonlocal integral elasticity. *Int J Mech Sci* 2017; 133: 639–650.
3. Iijima S. Helical microtubules of graphitic carbon. *Nature* 1991; 354: 56–58.
4. Demir C, Civalek O and Akgoz B. Free vibration analysis of carbon nanotubes based on shear deformable beam theory by discrete singular convolution technique. *Math Comput Appl* 2010; 15: 57–65.
5. Wagner HD, Lourie O, Feldman Y, et al. Stress-induced fragmentation of multiwall carbon nanotubes in a polymer matrix. *Appl Phys Lett* 1998; 72: 188–190.
6. Thostenson ET, Ren Z and Chou TW. Advances in the science and technology of carbon nanotubes and their composites: a review. *Compos Sci Technol* 2001; 61: 1899–1912.
7. Qian D, Wagner GJ, Liu WK, et al. Mechanics of carbon nanotubes. *Appl Mech Rev* 2002; 55: 495–533.
8. Sirtori C. Applied physics: bridge for the terahertz gap. *Nature* 2002; 417: 132.
9. Antonelli GA, Maris HJ, Malhotra SG, et al. Picosecond ultrasonics study of the vibrational modes of a nanostructure. *J Appl Phys* 2002; 91: 3261–3267.
10. Brauns EB, Madaras ML, Coleman RS, et al. Complex local dynamics in DNA on the picosecond and nanosecond time scales. *Phys Rev Lett* 2002; 88: 158101.
11. Stankovich S, Dikin DA, Dommett GH, et al. Graphene-based composite materials. *Nature* 2006; 442: 282.
12. Lau KT, Gu C and Hui D. A critical review on nanotube and nanotube/nanoclay related polymer composite materials. *Compos Part B Eng* 2006; 37: 425–436.
13. Schedin F, Geim AK, Morozov SV, et al. Detection of individual gas molecules adsorbed on graphene. *Nat Mater* 2007; 6: 652.
14. Bunch JS, Van Der Zande AM, Verbridge SS, et al. Electromechanical resonators from graphene sheets. *Science* 2007; 315: 490–493.
15. Chiu HY, Hung P, Postma HWC, et al. Atomic-scale mass sensing using carbon nanotube resonators. *Nano Lett* 2008; 8: 4342–4346.
16. Arash B and Wang Q. A review on the application of nonlocal elastic models in modeling of carbon nanotubes and graphenes. *Comput Mater Sci* 2012; 51: 303–313.
17. Murmu T, Adhikari S and Wang CY. Torsional vibration of carbon nanotubebuckyball systems based on nonlocal elasticity theory. *Phys E Low Dimens Syst Nanostruct* 2011; 43: 1276–1280.
18. Dai H, Hafner JH, Rinzler AG, et al. Nanotubes as nanoprobes in scanning probe microscopy. *Nature* 1996; 384: 147.
19. Bachtold A, Hadley P, Nakanishi T, et al. Logic circuits with carbon nanotube transistors. *Science* 2001; 294: 1317–1320.
20. Kim P and Lieber CM. Nanotube nanotweezers. *Science* 1999; 286: 2148–2150.
21. Thostenson ET, Ren Z and Chou TW. Advances in the science and technology of carbon nanotubes and their composites: a review. *Compos Sci Technol* 2001; 61: 1899–1912.
22. Mehdipour I and Barari A. Why the center-point of bridged carbon nanotube length is the most mass sensitive location for mass attachment? *Comput Mater Sci* 2012; 55: 136–141.
23. Joshi AY, Harsha SP and Sharma SC. Vibration signature analysis of single walled carbon nanotube based nanomechanical sensors. *Phys E Low Dimens Syst Nanostruct* 2010; 42: 2115–2123.
24. Chien WT, Chen CS and Chen HH. Resonant frequency analysis of fixed-free single-walled carbon nanotube-based mass sensor. *Sens Actuators A Phys* 2006; 126: 117–121.

25. Arroyo M and Belytschko T. Continuum mechanics modeling and simulation of carbon nanotubes. *Meccanica* 2005; 40: 455–469.
26. Wan H and Delale F. A structural mechanics approach for predicting the mechanical properties of carbon nanotubes. *Meccanica* 2010; 45: 43–51.
27. Chowdhury R, Adhikari S and Mitchell J. Vibrating carbon nanotube based bio-sensors. *Phys E Low Dimens Syst Nanostruct* 2009; 42: 104–109.
28. Yayli MO and Cercevik AE. 1725. Axial vibration analysis of cracked nanorods with arbitrary boundary conditions. *J Vibroeng* 2015; 17.
29. Barretta R, Brcic M, Canadija M, et al. Application of gradient elasticity to armchair carbon nanotubes: size effects and constitutive parameters assessment. *Eur J Mech A/Solids* 2017; 65: 1–13.
30. El-Borgi S, Rajendran P, Friswell MI, et al. Torsional vibration of size-dependent viscoelastic rods using nonlocal strain and velocity gradient theory. *Compos Struct* 2018; 186: 274–292.
31. Polizzotto C. Stress gradient versus strain gradient constitutive models within elasticity. *Int J Solids Struct* 2014; 51: 1809–1818.
32. Polizzotto C. A unifying variational framework for stress gradient and strain gradient elasticity theories. *Eur J Mech A/Solids* 2015; 49: 430–440.
33. Fernandez-Saez J and Zaera R. Vibrations of Bernoulli-Euler beams using the two-phase nonlocal elasticity theory. *Int J Eng Sci* 2017; 119: 232–248.
34. Mahmoud FF. On the nonexistence of a feasible solution in the context of the differential form of Eringens constitutive model: a proposed iterative model based on a residual nonlocality formulation. *Int J Appl Mech* 2017; 9: 1750094.
35. Filiz S and Aydogdu M. Axial vibration of carbon nanotube heterojunctions using nonlocal elasticity. *Comput Mater Sci* 2010; 49: 619–627.
36. Aydogdu M. Axial vibration of the nanorods with the nonlocal continuum rod model. *Phys E Low Dimens Syst Nanostruct* 2009; 41: 861–864.
37. Peddieson J, Buchanan GR and McNitt RP. Application of nonlocal continuum models to nanotechnology. *Int J Eng Sci* 2003; 41: 305–312.
38. Sudak LJ. Column buckling of multiwalled carbon nanotubes using nonlocal continuum mechanics. *J Appl Phys* 2003; 94: 7281–7287.
39. Reddy JN. Nonlocal theories for bending, buckling and vibration of beams. *Int J Eng Sci* 2007; 45: 288–307.
40. Lu P, Lee HP, Lu C, et al. Application of nonlocal beam models for carbon nanotubes. *Int J Solids Struct* 2007; 44: 5289–5300.
41. Heireche H, Tounsi A, Benzair A, et al. Sound wave propagation in single-walled carbon nanotubes with initial axial stress. *J Appl Phys* 2008; 104: 014301.
42. Lim CW and Yang Y. New predictions of size-dependent nanoscale based on nonlocal elasticity for wave propagation in carbon nanotubes. *J Comput Theor Nanosci* 2010; 7: 988–995.
43. Shen HS. Nonlinear vibration of microtubules in living cells. *Curr Appl Phys* 2011; 11: 812–821.
44. Demir C and Civalek O. Torsional and longitudinal frequency and wave response of microtubules based on the nonlocal continuum and nonlocal discrete models. *Appl Math Modell* 2013; 37: 9355–9367.
45. Zhang YQ, Liu GR and Xie XY. Free transverse vibrations of double-walled carbon nanotubes using a theory of nonlocal elasticity. *Phys Rev B* 2005; 71: 195404.
46. Lu P, Lee HP, Lu C, et al. Dynamic properties of flexural beams using a nonlocal elasticity model. *J Appl Phys* 2006; 99: 073510.
47. Islam ZM, Jia P and Lim CW. Torsional wave propagation and vibration of circular nanostructures based on nonlocal elasticity theory. *Int J Appl Mech* 2014; 6: 1450011.
48. Pradhan SC and Murmu T. Differential quadrature method for vibration analysis of beam on Winkler foundation based on nonlocal elastic theory. *J Inst Eng (India) Metallurgy Mater Eng Div* 2009; 89: 3–12.
49. Wang CM, Kitipornchai S, Lim CW, et al. Beam bending solutions based on nonlocal Timoshenko beam theory. *J Eng Mech* 2008; 134: 475–481.
50. Zhang YQ, Liu GR and Wang JS. Small-scale effects on buckling of multiwalled carbon nanotubes under axial compression. *Phys Rev B* 2004; 70: 205430.
51. Loya JA, Aranda-Ruiz J and Fernndez-Sez J. Torsion of cracked nanorods using a nonlocal elasticity model. *J Phys D Appl Phys* 2014; 47: 115304.
52. Rahmani O, Hosseini SAH, Noroozi Moghaddam MH, et al. Torsional vibration of cracked nanobeam based on nonlocal stress theory with various boundary conditions: an analytical study. *Int J Appl Mech* 2015; 7: 1550036.
53. Nazemnezhad R and Fahimi P. Free torsional vibration of cracked nanobeams incorporating surface energy effects. *Appl Math Mech* 2017; 38: 217–230.
54. Barretta R, Diaco M, Feo L, et al. Stress-driven integral elastic theory for torsion of nano-beams. *Mech Res Commun* 2017; 87: 35–41.

55. Apuzzo A, Barretta R, Canadija M, et al. A closed-form model for torsion of nanobeams with an enhanced nonlocal formulation. *Compos Part B Eng* 2017; 108: 315–324.
56. Barretta R and de Sciarra FM. Analogies between nonlocal and local BernoulliEuler nanobeams. *Arch Appl Mech* 2015; 85: 89–99.
57. Polizzotto C. Variational formulations and extra boundary conditions within stress gradient elasticity theory with extensions to beam and plate models. *Int J Solids Struct* 2016; 80: 405–419.
58. Barretta R and Marotti de Sciarra F. A nonlocal model for carbon nanotubes under axial loads. *Adv Mater Sci Eng* 2013.
59. Yayli MO. Buckling analysis of Euler columns embedded in an elastic medium with general elastic boundary conditions. *Mech Based Des Struct Mach* 2018; 46: 110–122.
60. Yayli MO. A compact analytical method for vibration analysis of single-walled carbon nanotubes with restrained boundary conditions. *J Vib Control* 2016; 22: 2542–2555.
61. Yayli MO. A compact analytical method for vibration of micro-sized beams with different boundary conditions. *Mech Adv Mater Struct* 2017; 24: 496–508.
62. Eringen AC and Edelen DGB. On nonlocal elasticity. *Int J Eng Sci* 1972; 10: 233–248.
63. Romano G, Barretta R, Diaco M, et al. Constitutive boundary conditions and paradoxes in nonlocal elastic nanobeams. *Int J Mech Sci* 2017; 121: 151–156.
64. Barretta R, Canadija M, Feo L, et al. Exact solutions of inflected functionally graded nano-beams in integral elasticity. *Compos Part B Eng* 2017; 142: 273–286.
65. Yayli MO. On the axial vibration of carbon nanotubes with different boundary conditions. *Micro Nano Lett* 2014; 9: 807–811.
66. Yayli MO. Stability analysis of gradient elastic microbeams with arbitrary boundary conditions. *J Mech Sci Technol* 2015; 29: 3373–3380.